Port-Hamiltonian Modeling of Hydraulics in 4th Generation District Heating Networks

Felix Strehle, Juan E. Machado, Michele Cucuzzella, Albertus J. Malan, Jacquelien M.A. Scherpen, and Sören Hohmann

Abstract— In this paper, we use elements of graph theory and port-Hamiltonian systems to develop a modular dynamic model describing the hydraulic behavior of 4th generation district heating networks. In contrast with earlier generation networks with a single or few heat sources and pumps, newer installations will prominently feature distributed heat generation units, bringing about a number of challenges for the control and stable operation of these systems, e.g., flow reversals and interactions among pumps controllers, which may lead to severe oscillations. We focus thus on flexible system setups with an arbitrary number of distributed heat sources and end-users interconnected through a meshed, multi-layer distribution network of pipes. Moreover, differently from related works on the topic, we incorporate dynamic models for the pumps in the system and explicitly account for the presence of pressure holding units. By inferring suitable (power-preserving) interconnection ports, we provide a number of claims about the passivity properties of the overall, interconnected system, which proves to be highly beneficial in the design of decentralized control schemes and stability analyses.

Index terms: Modeling; Networked control systems; Port-Hamiltonian systems; District heating networks; Energy systems.

I. INTRODUCTION

District heating networks (DHNs) are a key element for a holistic energy transition, particularly in densely populated areas [1]–[4]. For their operation, well-defined, stable pressures and volume flow rates, i.e., hydraulic conditions, are a fundamental requirement as they form the basis for the actual heat power flows [3], [5]. Particularly in the transient regime, i.e., seconds after a disturbance or alteration of desired operation points, the hydraulic processes govern the system dynamics [5], [6].

In the operation of traditional 2nd or 3rd generation DHNs, the hydraulics and the thermal power flows are well-understood. Originating from a few main heat sources with large circulation pumps, the heat power flows follow decreasing pressure levels along the supply pipe layer to the end-user substations and back via the return pipe layer (see e.g.,

F. Strehle, A.J. Malan, S. Hohmann are with the Institute of Control Systems, Karlsruhe Institute of Technology (KIT), 76131, Karlsruhe, Germany. `felix.strehle@kit.edu`, `albertus.malan@kit.edu`, `soeren.hohmann@kit.edu`

J.E. Machado, M. Cucuzzella J.M.A. Scherpen are with the Jan C. Willems Center for Systems and Control, ENTEG, Faculty of Science and Engineering, University of Groningen, Nijenborgh 4, 9747 AG Groningen, the Netherlands. `j.e.machado.martinez(j.m.a.scherpen)@rug.nl`

M. Cucuzzella is also with the Department of Electrical, Computer and Biomedical Engineering, University of Pavia, via Ferrata 5, 27100 Pavia, Italy. `michele.cucuzzella@unipv.it`

[7, pp. 52–54]). However, emerging 4th generation DHNs bring about new challenges that call for new strategies and methods of operating, controlling and analyzing DHNs [1]–[3], [8], [9].[1] Most prominently, we see a rising integration of small pumps distributed throughout future DHNs. Primarily, this is due to the utilization of ever more distributed heat generation units (DGUs) such as heat pumps, combined heat and power, waste/biomass-to-energy, solar and geothermal heat plants, and waste heat recycling [1], [2]. Furthermore, supply/return temperatures are being decreased from around 80 °C–120 °C/40 °C–70 °C in 2nd or 3rd generation DHNs to 40 °C–70 °C/20 °C–40 °C in 4th generation DHNs [1], [3][10, pp. 33,59][7, p. 44]. One the one hand, this allows for the efficient integration of renewable heat sources and new consumers (e.g., low-energy buildings). On the other hand, together with decreasing pipe diameters, lower temperatures reduce the heat distribution losses. However, lower temperatures and smaller pipes require higher volume flow rates to carry the same amount of energy, which leads to higher pressure losses. This in turn requires additional pumps, which are typically added at end-user substations (see e.g. [1], [11]).

Additionally, the results of [4], [12] and the references therein have shown that a distributed pump setup, in which pumps are installed at every DGU and end-user substation, has considerable potential to reduce the overall electrical energy required to operate DHN pumps. On top of that, closed, hydraulic circuits such as DHNs require so-called pressure holding (or pressure control) units [4] [7, pp. 54–55]. In DHNs, these are typically pressure dictation pumps located between a container and the DHN (see [13, Fig. 1]). They compensate volume changes due to temperature variations and keep the pressures in the network within permissible limits. Particularly at the suction side of DGU circulation pumps, a minimum pressure must be ensured to avoid damaging the pumps through cavitation [14].

From a control point of view, the integration of distributed pumps in DGUs, end-users, and pressure holding units introduces more diverse and complex pressure and volume flow dynamics. We see, e.g., more frequent volume flow reversals in pipes [15], [16] or interactions between the pump controllers, which may lead to severe hydraulic oscillations [4], [12], [14]. Furthermore, DGUs and thus their pumps naturally show intermittent operational behavior [2], [17]. Besides that, the classical two-layer supply and return pipe network topology can be extended in future DHNs

---

[1]See [1] for a comparison and overview of the different DHN generations.

by additional layers (see e.g., [10]). The return pipes of a traditional DHN may then serve as the supply for a new DHN part which, e.g., supplies low-energy buildings.

Upon closer examination, it becomes evident that the discussion above shows parallels to the trends and challenges in future power systems, particularly to the prominent microgrid paradigm (see, e.g., [18] or the discussion in [8]). Thus, it seems promising to follow the established view of the microgrid and power system control community and focus on decentralized control designs for novel pressure and volume flow rate controllers.[2] A major means of designing decentralized controllers are passivity-based designs (cf. [19]–[21]). As illustrated for example in recent works on microgrids [22]–[25], the compositional properties of passive systems provide a promising framework for control that can cope with complex, frequently changing network topologies and dynamically interacting subsystems and controllers, respectively. Due to their inherent passivity properties and port perspective, which gives a clear understanding of how subsystems interact with each other, port-Hamiltonian system (PHS) models are a natural starting point for such passivity-based, decentralized controller designs (see [19], [20], [22], [26]).

In the literature, the field of port-Hamiltonian modeling of DHNs is largely unexplored. In [8], first results are given that model the hydraulic dynamics of DGUs, end-users, and pipes as input-state-output PHS (ISO-PHS). In [27], a comprehensive PDE-based thermohydraulic, spatially-discretized port-Hamiltonian model of DHNs is proposed. In [28], a PHS model of the thermal dynamics in an electro-thermal microgrid is developed. General dynamic models to describe the hydraulic behavior of DHNs have been developed in [11], [29] for systems with one heat source (see also [27]), and in [9], [30] for systems with multiple, distributed sources. Nevertheless, none of these references consider pressure holding units nor dynamic pump models.

Therefore, in this work, we set the basis for decentralized pressure and volume flow rate control designs by providing a comprehensive dynamic, hydraulic PHS model of a 4th generation DHN with flexible topology. Specifically, we allow for an arbitrary number of DGUs and end-users to be connected via a flexible, multi-layer pipe network topology. We extend existing hydraulic DHN models (see, e.g., [8], [9], [11], [29], [31]) by considering dynamic models for the circulation pumps as well as for the pressure holding units. Inspired by practically oriented results (see, e.g., [32]), we use linear second-order models to represent both the pressure holding and the circulation pump dynamics. For all subsystem models, we give explicit input-state-output port-Hamiltonian system (ISO-PHS) representations. From the ISO-PHS models, we deduce some inherent properties of the overall DHN model such as a power-preserving subsystem interconnection structure and passivity. These properties pave

the way to designing pressure and volume flow rate controllers that asymptotically stabilize desired hydraulic equilibria in 4th generation DHNs with flexible topologies.[3]

II. MODELING

In this section, we model the hydraulics of a general class of 4th generation DHNs with flexible topologies comprising pipes connecting an arbitrary number of DGUs and end-users. First, we formally describe the DHN as a weakly connected digraph. Afterwards, we present the models of the three main subsystems: *DGU*, *end-user*, and *pipe*. In contrast to existing models (see e.g., [8], [9], [11], [29], [31]), we extend the DGU and end-user models by dynamic, linear, second-order pump models and add a pressure holding unit to each DGU. For the modeling, we make the following assumptions which are valid under normal operating conditions (see [6], [11]):

Assumption 1: The compressibility of water is neglected. Any reference and nominal pressure values as well as all model parameters are strictly positive. Pressure losses inside pipes $\lambda(q)$ and valves $\mu(q, s_v)$ are continuously differentiable ($\mathcal{C}^1$) functions that are strictly monotonically increasing with $\lambda(0) = 0$ and $\mu(0, s_v) = 0$ for all valve stem positions s_v, respectively.

A. Digraph representation of a DHN

We describe a DHN as a weakly connected digraph $\mathcal{G} = (\mathcal{V}, \mathcal{E})$ without self-loops as shown in Fig. 1. The edges $\mathcal{E}$ are partitioned into three sets: $\mathcal{D} = \{1, \ldots, D\}, D \geq 1$, represents the DGUs, $\mathcal{L} = \{D+1, \cdots, D+L\}, L \geq 1$, the end-users (loads), and $\mathcal{P} = \{D+L+1, \cdots, D+L+P\}, P \geq 2$, the pipes. For each node $a \in \mathcal{V}$, $\mathcal{N}_a^+ = \{(x,y) \in \mathcal{E} : y = a\}$ and $\mathcal{N}_a^- = \{(x,y) \in \mathcal{E} : x = a\}$ denote the sets of edges incoming/outgoing to/from a, respectively. For edge $j = 4 = (3, 7)$ in Fig. 1, which represents end-user 4, we for example get the sets of incoming and outgoing edges at tail $a = 3 \in \mathcal{V}$, $\mathcal{N}_3^+ = \{((2,3) = 8)\}$, $\mathcal{N}_3^- = \{(3,4) = 9\}$ and at head $b = 7 \in \mathcal{V}$, $\mathcal{N}_7^+ = \{(8,7) = 12, (11,7) = 15\}$, $\mathcal{N}_7^- = \{(7,6) = 11\}$. The nodes correspond to ideal connection points of the DGUs and end-users to the pipe network of the DHN. Thus, all volume flow rates at a node $c \in \mathcal{V}$ sum up to zero. This can be understood as a generalized version of Kirchhoff's current law (KCL) (see [33, p. 126]). Furthermore, DGUs and end-users are always connected via pipes and never directly connect to the same node. That is, all nodes $a, b \in \mathcal{V}$ that are tails or heads of edges $(a, b) \in \mathcal{D} \cup \mathcal{L}$, are connected via edges $l \in \mathcal{P}$ (see Fig. 1). The orientation of the edges represents the reference direction of positive flows.

B. Hydraulic DGU Model with Pressure Holding

The hydraulic DGU circuit at an edge $i = (a, b) \in \mathcal{D}$ in the DHN comprises two main parts (see Fig. 2): a pressure holding unit (red) (see [7, pp. 54–55]) and a circulation circuit (black/blue) (see [34], [35]).
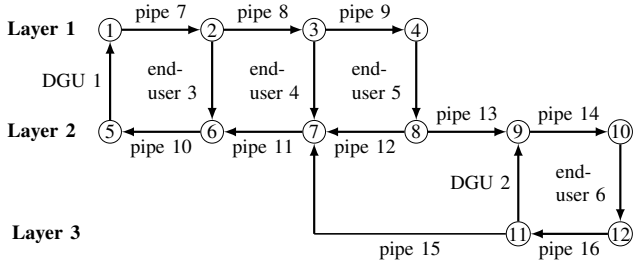
Fig. 1. Digraph representation of an exemplary DHN containing 2 DGUs $\mathcal{D} = \{1, 2\}$, 4 end-users $\mathcal{L} = \{3, 4, 5, 6\}$, and 10 pipes $\mathcal{P} = \{7, \ldots, 16\}$ in a three-layer topology; the 12 nodes $\mathcal{V} = \{1, \ldots, 12\}$ represent simple hydraulic connection points at which the sum of all volume flow rates is zero
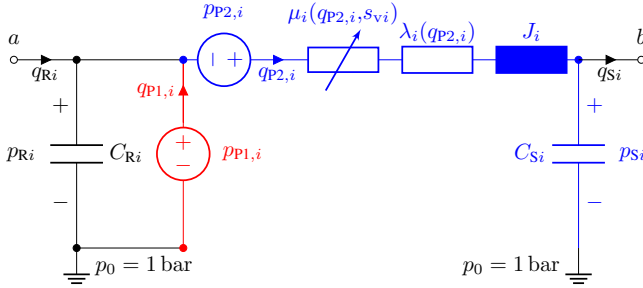
Fig. 2. Equivalent circuit of a hydraulic DGU model with pressure holding (red) and circulation circuit (black/blue); without loss of generality, the capacitance $C_{\mathrm{R}i}$ may be lumped with the pressure holding (see Section II-B.3)

1) Dynamic Pump Model: In both the pressure holding and the circulation circuit, pumps are essential components. In prevalent literature (see e.g., [4], [8], [9], [11], [12], [29], [31]), pumps are usually considered as ideal pressure sources modeled by a voltage source in the equivalent circuit diagram as illustrated in Fig. 2. However, the dynamics of pumps, particularly the ones of centrifugal pumps widely used in DHNs [11], [36], lie in the range of several hundred ms (see [32, Fig. 8–9]). As this is a time scale comparable to that of the overall DHN hydraulics (see [3], [6]), a more accurate control design and system analysis can be performed if pump dynamics are considered as well.

We note that in practice, the actual control input of a pump system is a desired rotational speed, which enters into an

---

[3] Summaries of the abbreviations and symbols used in this paper appear in Appendices I and II, respectively.
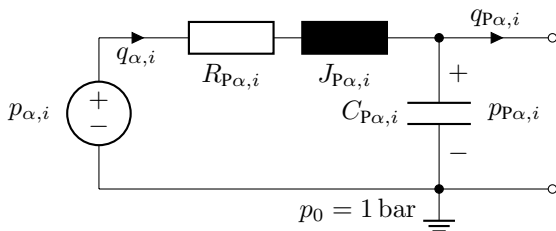
Fig. 3. Equivalent circuit of a linear, second-order approximation of pump dynamics (cf. [32]).

automatic speed control of the AC motor driving the pump [37, pp. 28,51]. In this work, we suggest approximating the dynamics arising from the complex arrangement of power electronics, speed-controlled AC motor, and pump hydraulics by a linear second-order system. The linear second-order system relates some kind of input pressure $p_{\alpha,i}$, which results from the quadratic dependency on the rotational speed set point $p_{\alpha,i} \propto (\omega_\alpha^*)^2$, to the actual output pressure $p_{\mathrm{P}\alpha,i}$ of the pump (see [32]). The corresponding actual output volume flow rate of the pump is $q_{\mathrm{P}\alpha,i}$.

The above can be understood as a linear RLC circuit as illustrated in Fig. 3. The parameters $R_{\mathrm{P}\alpha}$, $J_{\mathrm{P}\alpha}$, and $C_{\mathrm{P}\alpha}$ are pure black box parameters without physical meaning. This is due to the fact that in the RLC circuit representation, the speed control and AC motor dynamics are merged with the hydraulic pump dynamics comprising fluid mass inertia, pressure losses, and hydraulic capacitance due to fluid compressibility and fluid volume (see e.g., [32]). By applying Kirchhoff's voltage law (KVL) and KCL to Fig. 3, we obtain the dynamics

$$J_{\mathrm{P}\alpha,i}\dot{q}_{\alpha,i} = -p_{\mathrm{P}\alpha,i} - R_{\mathrm{P}\alpha,i}q_{\mathrm{P}\alpha,i} + p_{\alpha,i},$$
$$C_{\mathrm{P}\alpha,i}\dot{p}_{\mathrm{P}\alpha,i} = q_{\alpha,i} - q_{\mathrm{P}\alpha,i}, \tag{1}$$

which may be written in linear ISO-PHS form (see [38, p. 116]) as follows:

$$\dot{x}_{\mathrm{P}\alpha,i} = [J_{\mathrm{P}\alpha,i} - R_{\mathrm{P}\alpha,i}]\frac{\partial H_{\mathrm{P}\alpha,i}(x_{\mathrm{P}\alpha,i})}{\partial x_{\mathrm{P}\alpha,i}}$$
$$+ G_{\mathrm{P}\alpha,i}u_{\mathrm{P}\alpha,i} + K_{\mathrm{P}\alpha,i}d_{\mathrm{P}\alpha,i}, \tag{2a}$$

$$y_{\mathrm{P}\alpha,i} = G_{\mathrm{P}\alpha,i}^{\mathsf{T}}\frac{\partial H_{\mathrm{P}\alpha,i}(x_{\mathrm{P}\alpha,i})}{\partial x_{\mathrm{P}\alpha,i}}, \tag{2b}$$

$$z_{\mathrm{P}\alpha,i} = K_{\mathrm{P}\alpha,i}^{\mathsf{T}}\frac{\partial H_{\mathrm{P}\alpha,i}(x_{\mathrm{P}\alpha,i})}{\partial x_{\mathrm{P}\alpha,i}}, \tag{2c}$$

$$H_{\mathrm{P}\alpha,i}(x_{\mathrm{P}\alpha,i}) = \frac{1}{2}x_{\mathrm{P}\alpha,i}^{\mathsf{T}}\underbrace{\mathrm{Diag}\left[\frac{1}{J_{\mathrm{P}\alpha,i}}, \frac{1}{C_{\mathrm{P}\alpha,i}}\right]}_{Q_{\mathrm{P}\alpha,i}}x_{\mathrm{P}\alpha,i}. \tag{2d}$$

In (2), the states and co-states are given by

$$x_{\mathrm{P}\alpha,i} = [J_{\mathrm{P}\alpha,i}q_{\alpha,i}, C_{\mathrm{P}\alpha,i}p_{\mathrm{P}\alpha,i}]^{\mathsf{T}} \tag{2e}$$

and

$$\frac{\partial H_{\mathrm{P}\alpha,i}(x_{\mathrm{P}\alpha,i})}{\partial x_{\mathrm{P}\alpha,i}} = Q_{\mathrm{P}\alpha,i}x_{\mathrm{P}\alpha,i} = [q_{\alpha,i}, p_{\mathrm{P}\alpha,i}]^{\mathsf{T}}, \tag{2f}$$

respectively. The control port pair is $(u_{\mathrm{P}\alpha,i} = p_{\alpha,i}, y_{\mathrm{P}\alpha,i} = q_{\alpha,i})$. The uncontrolled interaction (coupling) port pair is

$$(d_{\mathrm{P}\alpha,i} = -q_{\mathrm{P}\alpha,i}, \; z_{\mathrm{P}\alpha,i} = p_{\mathrm{P}\alpha,i}). \tag{2g}$$

The interconnection matrix, the damping matrix, the input matrix, and the interaction matrix are given by

$$J_{\mathrm{P}\alpha,i} = \begin{bmatrix} 0 & -1 \\ 1 & 0 \end{bmatrix}, \; R_{\mathrm{P}\alpha,i} = \begin{bmatrix} R_{\mathrm{P}\alpha,i} & 0 \\ 0 & 0 \end{bmatrix}, \tag{2h}$$

$G_{\mathrm{P}\alpha,i} = [1, 0]^{\mathsf{T}}$, and $K_{\mathrm{P}\alpha,i} = [0, 1]^{\mathsf{T}}$, respectively. Thus, in the following, we consider the red and blue voltage sources in Fig. 2 to represent RLC circuits as given in Fig. 3. For

the pressure holding, we set $\alpha = 1$. For the circulation pump in the circulation circuit, we set $\alpha = 2$.

Remark 1: In practice, the parameters $R_{P\alpha}$, $J_{P\alpha}$, and $C_{P\alpha}$ can be identified from measurement data obtained by operating the pump in typical scenarios. Alternatively, they could be fitted in simulations to match characteristic curves provided in data sheets. However, we note that some robust control schemes may not require such knowledge of the plant parameters (see, e.g., passivity-based control [24]).

2) Circulation Circuit Model: The equivalent circuit diagram of the hydraulic circulation circuit is illustrated in black and blue in Fig. 2. It comprises a serial connection of a circulation pump, a control valve, pipes, and a heat exchanger (see [34], [35]). All pipes are described by nonlinear, volume flow-dependent resistances $\lambda_i(q_{P2,i})$ and inductances J_i which represent the pipe friction and volume inertia, respectively. The control valve is modeled as a nonlinear resistance $\mu_i(q_{P2,i}, s_{vi})$ with an adjustable parameter s_{vi}. The two capacitances C_{Ri}, C_{Si} represent the hydraulic elasticity of the components in the DGU circulation circuit. Note that heat exchangers contribute significantly to these elasticities (see [39], [40]). To simplify the situation, we may, without loss of generality, consider the capacitance C_{Ri} to be lumped with $C_{P1,i}$ from the dynamic pump model (replace the red voltage source in Fig. 2 with Fig. 3 and set $\alpha = 1$). The circulation pump is modeled as a linear second-order system of form (2) with $\alpha = 2$, whose interaction with the circulation circuit is represented by the blue voltage source. The pressures p_{Ri}, p_{Si} are the connection pressures at the return and supply side of a DGU with corresponding return inflow q_{Ri} and supply outflow q_{Si}.

By applying KVL and KCL to the blue part in Fig. 2, we obtain the dynamics

$$J_i \dot{q}_{P2,i} = -p_{Si} - \lambda_i(q_{P2,i}) - \mu_i(q_{P2,i}, s_{vi}) + p_{P2,i} + p_{P1,i},$$
$$C_{Si} \dot{p}_{Si} = q_{P2,i} - q_{Si}, \tag{3}$$

which may be written as an ISO-PHS with a nonlinear resistive structure (see [38, p. 114]) as follows:

$$\dot{x}_i = J_i \frac{\partial H_i(x_i)}{\partial x_i} - \mathcal{R}_i(x_i) + K_i d_i, \tag{4a}$$

$$z_i = K_i^\mathsf{T} \frac{\partial H_i(x_i)}{\partial x_i}, \tag{4b}$$

$$H_i(x_i) = \frac{1}{2} x_i^\mathsf{T} \underbrace{\mathrm{Diag}\left[\frac{1}{J_i}, \frac{1}{C_{Si}}\right]}_{Q_i} x_i. \tag{4c}$$

In (4), the states and co-states are given by

$$x_i = [J_i q_{P2,i}, C_{Si} p_{Si}]^\mathsf{T} \tag{4d}$$

and

$$\frac{\partial H_i(x_i)}{\partial x_i} = Q_i x_i = [q_{P2,i}, p_{Si}]^\mathsf{T}, \tag{4e}$$

respectively. The interaction (coupling) input is

$$d_i = \begin{bmatrix} p_{P1,i} \\ p_{P2,i} \\ -q_{Si} \end{bmatrix} = \begin{bmatrix} p_{P1,i} \\ p_{P2,i} \\ \sum_{l \in \mathcal{N}_b^+} q_l - \sum_{l \in \mathcal{N}_b^-} q_l \end{bmatrix} \tag{4f}$$

and the corresponding conjugated output reads as

$$z_i = [q_{P1,i}, q_{P2,i}, p_{Si}]^\mathsf{T}. \tag{4g}$$

The interconnection matrix, the interaction matrix and the damping function are given by

$$J_i = \begin{bmatrix} 0 & -1 \\ 1 & 0 \end{bmatrix}, \quad K_i = \begin{bmatrix} 1 & 1 & 0 \\ 0 & 0 & 1 \end{bmatrix},$$
$$\mathcal{R}_i(x_i) = [\lambda_i(q_{P2,i}) + \mu_i(q_{P2,i}, s_{vi}), \quad 0]^\mathsf{T}, \tag{4h}$$

respectively. The interaction (coupling) between (2) with $\alpha = 2$ and (4) is established via

$$\begin{aligned} d_{2,i} = p_{P2,i} = z_{P2,i} \\ d_{P2,i} = -q_{P2,i} = -z_{2,i} \end{aligned} \Leftrightarrow \begin{bmatrix} d_{2,i} \\ d_{P2,i} \end{bmatrix} = \begin{bmatrix} 0 & 1 \\ -1 & 0 \end{bmatrix} \begin{bmatrix} z_{2,i} \\ z_{P2,i} \end{bmatrix}. \tag{5}$$

3) Pressure Holding Model: The pressure holding unit in DHNs is typically a dynamic pressure control conducted by a pressure dictation pump with an overflow valve located between a pressurized container and the DHN [7, pp. 54–55], [13, Fig. 1]. It is almost exclusively connected to the suction side of the circulation pump (pre-pressure control) (see Fig. 2) and is instrumental in preventing cavitation in the circulation pump [7, pp. 54–55], [14]. As outlined in Section II-B.1, we approximate the pump dynamics by a linear second-order system of form (2) with $\alpha = 1$. In the case of the pressure holding unit, we find it more convenient to think of the red voltage source in Fig. 2 as being replaced with the RLC circuit in Fig. 3, where $\alpha = 1$. That is, in contrast to the circulation pump, which still needs to be coupled with the circulation circuit (blue part in Fig. 2), the red voltage source already represents the entire pressure holding unit. For this, we consider the dictation pump to be lumped together with the pressurized container, and allow for the container to operate in both charging and discharging mode.

C. Hydraulic End-User Models

In future DHNs, additional pumps are expected to be included in end-user circuits. On the one hand, this allows to compensate higher pressure losses in the network due to smaller pipe diameters [1], [11]. On the other hand, results from [4], [12] and the references therein suggest that such a setup considerably reduces the electrical energy required to operate the pumps in DHNs. As a result, the hydraulic end-user circuit at an edge $j = (a, b) \in \mathcal{L}$ is modeled similarly to the hydraulic DGU circulation circuit in blue in Fig. 2 (see Fig. 4, [8, Fig. 2]). The only differences are the working direction of the pump and the sign conventions of the volume flow rates [7, pp. 87,143]. This allows for a more intuitive perspective of water flowing from the supply into end-users (q_{Sj}) and out at the return (q_{Rj}) for positive volume flow rate values. By applying KVL and KCL to Fig. 4, we obtain the dynamics

$$\begin{aligned} J_j \dot{q}_{P2,j} &= p_{Sj} - p_{Rj} - \lambda_j(q_{P2,j}) - \mu_j(q_{P2,j}, s_{vj}) + p_{P2,j}, \\ C_{Sj} \dot{p}_{Sj} &= -q_{P2,j} + q_{Sj}, \\ C_{Rj} \dot{p}_{Rj} &= q_{P2,j} - q_{Rj}, \end{aligned} \tag{6}$$
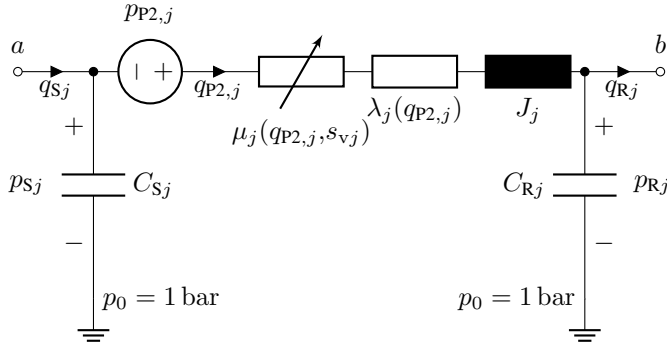
Fig. 4. Equivalent circuit of a hydraulic end-user model [8, Fig. 2]

which may be written as an ISO-PHS with a nonlinear resistive structure (see [38, p. 114]) as follows:

$$\dot{\boldsymbol{x}}_j = \boldsymbol{J}_j \frac{\partial H_j(\boldsymbol{x}_j)}{\partial \boldsymbol{x}_j} - \boldsymbol{\mathcal{R}}_j(\boldsymbol{x}_j) + \boldsymbol{K}_j \boldsymbol{d}_j, \qquad (7a)$$

$$\boldsymbol{z}_j = \boldsymbol{K}_j^{\mathsf{T}} \frac{\partial H_j(\boldsymbol{x}_j)}{\partial \boldsymbol{x}_j}, \qquad (7b)$$

$$H_j(\boldsymbol{x}_j) = \frac{1}{2} \boldsymbol{x}_j^{\mathsf{T}} \underbrace{\mathrm{Diag}\left[\frac{1}{J_j}, \frac{1}{C_{\mathrm{S}j}}, \frac{1}{C_{\mathrm{R}j}}\right]}_{\boldsymbol{Q}_j} \boldsymbol{x}_j. \qquad (7c)$$

In (7), the states and co-states are given by

$$\boldsymbol{x}_j = [J_j q_{\mathrm{P2},j}, C_{\mathrm{S}j} p_{\mathrm{S}j}, C_{\mathrm{R}j} p_{\mathrm{R}j}]^{\mathsf{T}} \qquad (7d)$$

and

$$\frac{\partial H_j(\boldsymbol{x}_j)}{\partial \boldsymbol{x}_j} = \boldsymbol{Q}_j \boldsymbol{x}_j = [q_{\mathrm{P2},j}, p_{\mathrm{S}j}, p_{\mathrm{R}j}]^{\mathsf{T}}, \qquad (7e)$$

respectively. Note that in this case both capacitors $C_{\mathrm{R}j}$ and $C_{\mathrm{S}j}$ are considered explicitly, as there is no pressure holding unit with which to lump them. The uncontrolled interaction (coupling) input is

$$\boldsymbol{d}_j = \begin{bmatrix} q_{\mathrm{S}j} \\ p_{\mathrm{P2},j} \\ -q_{\mathrm{R}j} \end{bmatrix} = \begin{bmatrix} \sum_{l \in \mathcal{N}_a^+} q_l - \sum_{l \in \mathcal{N}_a^-} q_l \\ p_{\mathrm{P2},j} \\ \sum_{l \in \mathcal{N}_b^+} q_l - \sum_{l \in \mathcal{N}_b^-} q_l \end{bmatrix} \qquad (7f)$$

and the corresponding conjugated output reads as $\boldsymbol{z}_j = [p_{\mathrm{S}j}, q_{\mathrm{P2},j}, p_{\mathrm{R}j}]^{\mathsf{T}}$. The interconnection matrix, the interaction matrix and the damping function are given by

$$\boldsymbol{J}_j = \begin{bmatrix} 0 & 1 & -1 \\ -1 & 0 & 0 \\ 1 & 0 & 0 \end{bmatrix}, \ \boldsymbol{K}_j = \begin{bmatrix} 0 & 1 & 0 \\ 1 & 0 & 0 \\ 0 & 0 & 1 \end{bmatrix},$$

$$\boldsymbol{\mathcal{R}}_j(\boldsymbol{x}_j) = [\lambda_j(q_{\mathrm{P2},j}) + \mu_j(q_{\mathrm{P2},j}, s_{\mathrm{v}j}), \ 0, \ 0]^{\mathsf{T}}, \qquad (7g)$$

respectively. The end-user pump is modeled similarly to the DGU circulation pump by a linear second-order system of form (2) with $i = j, \alpha = 2$. It is coupled to (7) via

$$\begin{aligned} d_{2,j} &= p_{\mathrm{P2},j} = z_{\mathrm{P2},j} \\ d_{\mathrm{P2},j} &= -q_{\mathrm{P2},j} = -z_{2,j} \end{aligned} \Leftrightarrow \begin{bmatrix} d_{2,j} \\ d_{\mathrm{P2},j} \end{bmatrix} = \begin{bmatrix} 0 & 1 \\ -1 & 0 \end{bmatrix} \begin{bmatrix} z_{2,j} \\ z_{\mathrm{P2},j} \end{bmatrix}. \quad (8)$$

Remark 2: To the best of our knowledge, pressure holding units as described for DGUs in Section II-B.3 are not used in end-user circuits. On the one hand, this makes sense from an
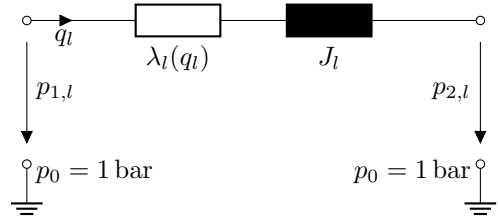
engineering perspective, as the suction side pressure of the end-user pump is the supply pressure. During feasible DHN operation, this supply pressure should always be sufficiently high to avoid any cavitation problems in the end-user pump. On the other hand, adding pressure holding units at every end-user would lead to unnecessary high implementation costs.

D. Hydraulic Pipe Model

For the hydraulic pipe model at an edge $l \in \mathcal{P}$, we directly follow the results of [8], [9], [11]. As illustrated in Fig. 5, we model the pipe friction by a nonlinear, volume flow-dependent resistance $\lambda_l(q_l)$ and the volume inertia by the linear inductance J_l. By applying KVL to Fig. 5, we obtain the dynamic equation

$$J_l \dot{q}_l = -\lambda_l(q_l) + p_{1,l} - p_{2,l} \qquad (9)$$

which may be written as an ISO-PHS model with a nonlinear resistive structure (see [38, p. 114]) as follows:

$$\dot{x}_l = -\mathcal{R}_l(x_l) + \boldsymbol{K}_l \boldsymbol{d}_l, \qquad (10a)$$

$$\boldsymbol{z}_l = \boldsymbol{K}_l^{\mathsf{T}} \frac{\partial H_l(x_l)}{\partial x_l}, \qquad (10b)$$

$$H_l(x_l) = \frac{1}{2J_l} x_l. \qquad (10c)$$

In (10), we have the state $x_l = J_l q_l$, the co-state $\frac{\mathrm{d}H_l(x_l)}{\mathrm{d}x_l} = q_l$, and the uncontrolled interaction (coupling) port pair

$$\left(\boldsymbol{d}_l = [p_{1,l}, p_{2,l}]^{\mathsf{T}}, \ \boldsymbol{z}_l = [q_l, -q_l]^{\mathsf{T}}\right). \qquad (10d)$$

The damping function and the interaction matrix are

$$\mathcal{R}_l(x_l) = \lambda_l(q_l), \quad \boldsymbol{K}_l = \begin{bmatrix} 1, & -1 \end{bmatrix}. \qquad (10e)$$

III. Model Properties

In this section, we highlight some inherent properties of the DHN model provided in Section II. In particular, we focus on properties that are beneficial for pressure and volume flow rate control of the pumps in the pressure holding and circulation circuits. Firstly, in Lemma 1, we show the power-preserving nature of the overall interconnection structure between the different DHN subsystem models developed in Section II. Then, in Subsection III-B, we make statements about the passivity properties of these DHN subsystem models. Together with the power-preserving interconnection structure, the inference of such passivity properties provide direct guidelines for pressure and volume flow rate control designs (see [41]).

Fig. 5. Equivalent circuit of a hydraulic pipe model [8, Fig. 3]

A. Interconnection Structure

The interconnection structure comprises two main parts: (i) the interconnection of DGUs $i \in \mathcal{D}$ and end-users $j \in \mathcal{L}$ to pipes $l \in \mathcal{P}$ at nodes $c \in \mathcal{V}$ in the DHN graph (see Fig. 1); (ii) the interconnection of the DGU and end-user circulation circuits (see Figs. 2 and 4) to their respective DGU circulation pump models ((2) with $\alpha = 2$) and end-user pump models ((2) with j instead of i and $\alpha = 2$). In the following Lemma, we show that the overall interconnection structure is power-preserving.

Lemma 1: Consider a DHN as described in Section II. The interconnections between DGUs $i \in \mathcal{D}$, end-users $j \in \mathcal{L}$, and pipes $l \in \mathcal{P}$ are power-preserving. Furthermore, the interconnection of a dynamic pump model with its respective DGU or end-user circulation circuit is power-preserving.

Proof: As outlined in Section II-A, the interconnection points of DGUs $i \in \mathcal{D}$ and end-user $j \in \mathcal{L}$ with their incoming and outgoing pipes, i.e., the nodes in $\mathcal{V}$, are ideal flow (volume flow rate) constraints that follow KCL. In detail, we get that at a tail node $a \in \mathcal{V}$ of a DGU edge $i = (a, b) \in \mathcal{D}$ the following holds (see (2g) and (4g)):

$$\begin{bmatrix} d_{1,i} \\ d_{\mathrm{P1},i} \\ \boldsymbol{d}_a^+ \\ \boldsymbol{d}_a^- \end{bmatrix} = \begin{bmatrix} 0 & 1 & 0 & 0 \\ -1 & 0 & -\mathbf{1}^\mathsf{T} & -\mathbf{1}^\mathsf{T} \\ 0 & \mathbf{1} & 0 & 0 \\ 0 & \mathbf{1} & 0 & 0 \end{bmatrix} \begin{bmatrix} z_{1,i} \\ z_{\mathrm{P1},i} \\ \boldsymbol{z}_a^+ \\ \boldsymbol{z}_a^- \end{bmatrix}, \quad (11)$$

with $\boldsymbol{d}_a^+ = \mathrm{col}\,(d_{2,l})_{l \in \mathcal{N}_a^+}$, $\boldsymbol{z}_a^+ = \mathrm{col}\,(z_{2,l})_{l \in \mathcal{N}_a^+}$, and $\boldsymbol{d}_a^- = \mathrm{col}\,(d_{1,l})_{l \in \mathcal{N}_a^-}$, $\boldsymbol{z}_a^- = \mathrm{col}\,(z_{1,l})_{l \in \mathcal{N}_a^-}$. Note that the pressure holding model, i.e., (2) with $\alpha = 1$, also enters here via its interaction port pair $d_{\mathrm{P1},i}, z_{\mathrm{P1},i}$ (see Fig. 2 and (2g)). At a head node $b \in \mathcal{V}$ of a DGU edge $i = (a, b) \in \mathcal{D}$, we get that

$$\begin{bmatrix} d_{3,i} \\ \boldsymbol{d}_b^+ \\ \boldsymbol{d}_b^- \end{bmatrix} = \begin{bmatrix} 0 & -\mathbf{1}^\mathsf{T} & -\mathbf{1}^\mathsf{T} \\ \mathbf{1} & 0 & 0 \\ \mathbf{1} & 0 & 0 \end{bmatrix} \begin{bmatrix} z_{3,i} \\ \boldsymbol{z}_b^+ \\ \boldsymbol{z}_b^- \end{bmatrix}, \quad (12)$$

with $\boldsymbol{d}_b^+ = \mathrm{col}\,(d_{2,l})_{l \in \mathcal{N}_b^+}$, $\boldsymbol{z}_b^+ = \mathrm{col}\,(z_{2,l})_{l \in \mathcal{N}_b^+}$ and $\boldsymbol{d}_b^- = \mathrm{col}\,(d_{1,l})_{l \in \mathcal{N}_b^-}$, $\boldsymbol{z}_b^- = \mathrm{col}\,(z_{1,l})_{l \in \mathcal{N}_b^-}$ (see Fig. 2). Analogously, we find that

$$\begin{bmatrix} d_{1,j} \\ \boldsymbol{d}_a^+ \\ \boldsymbol{d}_a^- \end{bmatrix} = \begin{bmatrix} 0 & -\mathbf{1}^\mathsf{T} & -\mathbf{1}^\mathsf{T} \\ \mathbf{1} & 0 & 0 \\ \mathbf{1} & 0 & 0 \end{bmatrix} \begin{bmatrix} z_{1,j} \\ \boldsymbol{z}_a^+ \\ \boldsymbol{z}_a^- \end{bmatrix} \quad (13)$$

and

$$\begin{bmatrix} d_{3,j} \\ \boldsymbol{d}_b^+ \\ \boldsymbol{d}_b^- \end{bmatrix} = \begin{bmatrix} 0 & -\mathbf{1}^\mathsf{T} & -\mathbf{1}^\mathsf{T} \\ \mathbf{1} & 0 & 0 \\ \mathbf{1} & 0 & 0 \end{bmatrix} \begin{bmatrix} z_{3,j} \\ \boldsymbol{z}_b^+ \\ \boldsymbol{z}_b^- \end{bmatrix} \quad (14)$$

hold at a tail node $a \in \mathcal{V}$ and a head node $b \in \mathcal{V}$ of an end-user edge $j = (a, b) \in \mathcal{L}$ (see Fig. 4). As the interconnection matrices in (11)–(14) are skew-symmetric, the interconnection structure represented by the nodes in $\mathcal{V}$ is power-preserving. The interconnection of a dynamic pump model with its respective circulation circuit model (4) and (7), respectively, is given by (see (5) and (8))

$$\begin{bmatrix} d_{\alpha,m} \\ d_{\mathrm{P}\alpha,m} \end{bmatrix} = \begin{bmatrix} 0 & 1 \\ -1 & 0 \end{bmatrix} \begin{bmatrix} z_{\alpha,m} \\ z_{\mathrm{P}\alpha,m} \end{bmatrix}. \quad (15)$$

with $\{m \in \mathcal{D}, \alpha = 1\} \cup \{m \in \mathcal{D} \cup \mathcal{L}, \alpha = 2\}$. As the interconnection matrix is skew-symmetric, the interconnection is power-preserving. The overall interconnection structure is thus a power-preserving Dirac structure [38, pp. 140], which satisfies

$$\begin{aligned} 0 = &\sum_{i \in \mathcal{D}} \left(\boldsymbol{z}_i^\mathsf{T} \boldsymbol{d}_i + z_{\mathrm{P1},i} d_{\mathrm{P1},i} + z_{\mathrm{P2},i} d_{\mathrm{P2},i} \right) \\ &+ \sum_{j \in \mathcal{L}} \left(\boldsymbol{z}_j^\mathsf{T} \boldsymbol{d}_j + z_{\mathrm{P2},j} d_{\mathrm{P2},j} \right) + \sum_{l \in \mathcal{P}} \boldsymbol{z}_l^\mathsf{T} \boldsymbol{d}_l. \end{aligned} \quad (16)$$

∎

B. Passivity of the Subsystem Models

Inferring passivity properties of the models for pumps (2), DGU circulation circuits (4), end-user circuits (7), and pipes (10) is straightforward in this case. As all models are represented in ISO-PHS form, they are all at least passive with respect to their Hamiltonians (storage functions) and their control and interaction ports [38, p. 116]. With Lemma 1, we can directly conclude that the overall hydraulic DHN model is passive as well. Its Hamiltonian is given by the sum of the positive definite Hamiltonians of the subsystems

$$\begin{aligned} H_{\mathrm{DHN}}(\boldsymbol{x}_{\mathrm{DHN}}) = &\sum_{i \in \mathcal{D}} \left(H_i(\boldsymbol{x}_i) + H_{\mathrm{P1},i}(\boldsymbol{x}_{\mathrm{P1},i}) + H_{\mathrm{P2},i}(\boldsymbol{x}_{\mathrm{P2},i}) \right) \\ &+ \sum_{j \in \mathcal{L}} \left(H_j(\boldsymbol{x}_j) + H_{\mathrm{P2},j}(\boldsymbol{x}_{\mathrm{P2},j}) \right) + \sum_{l \in \mathcal{P}} H_l(x_l) \end{aligned} \quad (17)$$

and is thus again positive definite. The time derivative of (17) satisfies

$$\dot{H}_{\mathrm{DHN}}(\boldsymbol{x}_{\mathrm{DHN}}) \leq \sum_{i \in \mathcal{D}} y_{\mathrm{P1},i} u_{\mathrm{P1},i} + \sum_{k \in \mathcal{D} \cup \mathcal{L}} y_{\mathrm{P2},k} u_{\mathrm{P2},k} \quad (18)$$

which makes $H_{\mathrm{DHN}}(\boldsymbol{x}_{\mathrm{DHN}})$ a Lyapunov function for $u_{\mathrm{P1},i} = u_{\mathrm{P2},k} = 0$ and thus ensures stability of the origin $\boldsymbol{x}_{\mathrm{DHN}}^* = \mathbf{0}$. Naturally, during real DHN operation, desired pressures and volume flow rates need to be asymptotically stabilized at DGUs and end-users, which implies a forced, nonzero equilibrium $\boldsymbol{x}_{\mathrm{DHN}}^* \neq \mathbf{0}$. To achieve this, control designs for the pressure holding and circulation pumps may have the following implications: (i) a change in the dynamics of system (2), i.e., the matrices $\boldsymbol{J}_{\mathrm{P}\alpha,i}, \boldsymbol{R}_{\mathrm{P}\alpha,i}$ and $\boldsymbol{J}_{\mathrm{P2},j}, \boldsymbol{R}_{\mathrm{P2},j}$, respectively; (ii) an extension of the system dynamics of (2) by adding integrator states; (iii) a shift of the equilibrium of (2) to desired pressure or volume flow rate values by modifying the Hamiltonian. However, in order to still allow for a modular stability analysis as outlined above, it is desired to preserve passivity with respect to the interaction port pairs $(d_{\mathrm{P}\alpha,i}, z_{\mathrm{P}\alpha,i})$ and $(d_{\mathrm{P2},j}, z_{\mathrm{P2},j})$, respectively (see also [8], [22]).

IV. CONCLUDING REMARKS

In this work, we have presented comprehensive ISO-PHS models that describe the dynamic behavior of the hydraulics in a general class of DHNs with flexible topologies. The models are capable of describing traditional DHNs as well as future DHNs with multiple distributed heat sources, pumps,

and multi-layer pipe network topologies. We extend prior works (e.g. [8], [9]) by explicitly considering the dynamics of pumps with a linear, second-order approximation and adding pressure holding units, which are essential for DHN operation. By means of the proposed digraph representation of a DHN in which the volume flow rates at nodes sum up to zero, as well as the ISO-PHS representation of the DHN subsystem models, we can readily infer passivity properties of the overall hydraulic DHN model and thus stability of its equilibrium. Particularly the clear understanding of interaction (coupling) ports provided by the ISO-PHS models and their inherent passivity properties prove to be highly beneficial. In future works, we will build upon these insights to design pressure and volume flow rate controllers to asymptotically stabilize desired hydraulic equilibria.

REFERENCES

[1] H. Lund, S. Werner, R. Wiltshire, S. Svendsen, J. E. Thorsen, F. Hvelplund, and B. V. Mathiesen, "4th Generation District Heating (4GDH): Integrating smart thermal grids into future sustainable energy systems," *Energy*, vol. 68, pp. 1–11, 2014.

[2] A. Vandermeulen, B. van der Heijde, and L. Helsen, "Controlling district heating and cooling networks to unlock flexibility: A review," *Energy*, vol. 151, pp. 103–115, 2018.

[3] N. N. Novitsky, Z. I. Shalaginova, A. A. Alekseev, V. V. Tokarev, O. A. Grebneva, A. V. Lutsenko, O. V. Vanteeva, E. A. Mikhailovsky, R. Pop, P. Vorobev, and M. Chertkov, "Smarter smart district heating," *Proceedings of the IEEE*, vol. 108, no. 9, pp. 1596–1611, 2020.

[4] H. Wang, H. Wang, and T. Zhu, "A new hydraulic regulation method on district heating system with distributed variable-speed pumps," *Energy Conversion and Management*, vol. 147, pp. 174–189, 2017.

[5] Z. Pan, Q. Guo, and H. Sun, "Interactions of district electricity and heating systems considering time-scale characteristics based on quasi-steady multi-energy flow," *Applied Energy*, vol. 167, pp. 230–243, 2016.

[6] M. Chertkov and N. N. Novitsky, "Thermal transients in district heating systems," *Energy*, vol. 184, pp. 22–33, 2019.

[7] T. Nussbaumer, S. Thalmann, A. Jenni, and J. Ködel, "Handbook on planning of district heating networks," QM Fernwärme and Energi-eSchweiz, 2020.

[8] F. Strehle, J. Vieth, M. Pfeifer, and S. Hohmann, "Passivity-based stability analysis of hydraulic equilibria in 4th generation district heating networks," *IFAC-PapersOnLine*, vol. 54, no. 19, pp. 261–266, 2021, 7th IFAC Workshop on Lagrangian and Hamiltonian Methods for Nonlinear Control LHMNC 2021.

[9] J. E. Machado, M. Cucuzzella, and J. M. Scherpen, "Modeling and passivity properties of multi-producer district heating systems," *Automatica*, vol. 142, 2022.

[10] H. Hertle, M. Pehnt, B. Gugel, M. Dingeldey, and K. Müller, *Wärmewende in Kommunen: Leitfaden für den klimafreundlichen Umbau der Wärmeversorgung (German) [Heat transition in municipalities: Guideline for a climate friendly change of heat supply]*, 3rd ed., ser. Schriften zur Ökologie. Berlin: Heinrich-Böll-Stiftung, 2015, vol. 41.

[11] C. de Persis and C. S. Kallesøe, "Pressure regulation in nonlinear hydraulic networks by positive and quantized controls," *IEEE Transactions on Control Systems Technology*, vol. 19, no. 6, pp. 1371–1383, 2011.

[12] A. Yan, J. Zhao, Q. An, Y. Zhao, H. Li, and Y. J. Huang, "Hydraulic performance of a new district heating systems with distributed variable speed pumps," *Applied Energy*, vol. 112, pp. 876–885, 2013.

[13] S. Buffa, M. H. Fouladfar, G. Franchini, I. Lozano Gabarre, and M. Andrés Chicote, "Advanced control and fault detection strategies for district heating and cooling systems—a review," *Applied Sciences*, vol. 11, no. 1, p. 455, 2021.

[14] T. Sommer, S. Mennel, and M. Sulzer, "Lowering the pressure in district heating and cooling networks by alternating the connection of the expansion vessel," *Energy*, vol. 172, pp. 991–996, 2019.

[15] B. van der Heijde, M. Fuchs, C. R. Tugores, G. Schweiger, K. Sartor, D. Basciotti, D. Müller, C. Nytsch-Geusen, M. Wetter, and L. Helsen, "Dynamic equation-based thermo-hydraulic pipe model for district heating and cooling systems," *Energy Conversion and Management*, vol. 151, pp. 158–169, 2017.

[16] J. Mohring, D. Linn, M. Eimer, M. Rein, and N. Siedow, "District heating networks–dynamic simulation and optimal operation," in *Mathematical Modeling, Simulation and Optimization for Power Engineering and Management*. Springer, 2021, pp. 303–325.

[17] A. De Lorenzi, A. Gambarotta, M. Morini, M. Rossi, and C. Saletti, "Setup and testing of smart controllers for small-scale district heating networks: An integrated framework," *Energy*, vol. 205, 2020.

[18] J. M. Guerrero, M. Chandorkar, T. Lee, and P. C. Loh, "Advanced control Aarchitectures for intelligent microgrids—part I: decentralized and hierarchical control," *IEEE Transactions on Industrial Electronics*, vol. 60, no. 4, pp. 1254–1262, 2013.

[19] R. Ortega and E. García-Canseco, "Interconnection and damping assignment passivity-based control: A survey," *European Journal of Control*, vol. 10, no. 5, pp. 432 – 450, 2004.

[20] B. Jayawardhana, R. Ortega, E. García-Canseco, and F. Castaños, "Passivity of nonlinear incremental systems: Application to pi stabilization of nonlinear rlc circuits," *Systems & Control Letters*, vol. 56, no. 9, pp. 618 – 622, 2007.

[21] R. Ortega, J. A. L. Perez, P. J. Nicklasson, and H. J. Sira-Ramirez, *Passivity-based control of Euler-Lagrange systems: mechanical, electrical and electromechanical applications*. Springer Science & Business Media, 2013.

[22] F. Strehle, P. Nahata, A. J. Malan, S. Hohmann, and G. Ferrari-Trecate, "A unified passivity-based framework for control of modular islanded ac microgrids," *IEEE Transactions on Control Systems Technology*, vol. 30, no. 5, pp. 1960–1976, 2022.

[23] J. D. Watson, Y. Ojo, K. Laib, and I. Lestas, "A scalable control design for grid-forming inverters in microgrids," *IEEE Transactions on Smart Grid*, vol. 12, no. 6, pp. 4726–4739, 2021.

[24] J. Ferguson, M. Cucuzzella, and J. M. Scherpen, "Exponential stability and local iss for dc networks," *IEEE Control Systems Letters*, vol. 5, no. 3, pp. 893–898, 2020.

[25] J. E. Machado and J. Schiffer, "A passivity-inspired design of power-voltage droop controllers for dc microgrids with electrical network dynamics," in *2020 59th IEEE Conference on Decision and Control (CDC)*. IEEE, 2020, pp. 3060–3065.

[26] A. van der Schaft, "Port-hamiltonian modeling for control," *Annual Review of Control, Robotics, and Autonomous Systems*, vol. 3, pp. 393–416, 2020.

[27] S.-A. Hauschild, N. Marheineke, V. Mehrmann, J. Mohring, A. M. Badlyan, M. Rein, and M. Schmidt, "Port-Hamiltonian Modeling of District Heating Networks," in *Progress in Differential-Algebraic Equations II*, ser. Differential-Algebraic Equations Forum. Cham: Springer International Publishing, 2020, pp. 333–355.

[28] A. Krishna and J. Schiffer, "A port-hamiltonian approach to modeling and control of an electro-thermal microgrid," *IFAC-PapersOnLine*, vol. 54, no. 19, pp. 287–293, 2021.

[29] T. Scholten, S. Trip, and C. De Persis, "Pressure regulation in large scale hydraulic networks with input constraints," *IFAC-PapersOnLine*, vol. 50, no. 1, pp. 5367–5372, 2017.

[30] S. Trip, T. Scholten, and C. D. Persis, "Optimal regulation of flow networks with transient constraints," *Automatica*, vol. 104, pp. 141–153, 2019.

[31] T. N. Jensen, "Plug and play control of hydraulic networks," Ph.D. dissertation, Aalborg University, Aalborg, 2012.

[32] F. Goppelt, T. Hieninger, and R. Schmidt-Vollus, "Modeling centrifugal pump systems from a system-theoretical point of view," in *2018 18th International Conference on Mechatronics - Mechatronika (ME)*, 2018, pp. 1–8.

[33] A. van der Schaft and D. Jeltsema, "Port-hamiltonian systems theory: an introductory overview," *Foundations and Trends in Systems and Control*, vol. 1, no. 2–3, pp. 173–378, 2014.

[34] G. Lennermo, P. Lauenburg, and S. Werner, "Control of decentralised solar district heating," *Solar Energy*, vol. 179, pp. 307–315, 2019.

[35] N. Lamaison, R. Bavière, D. Cheze, and C. Paulus, "A multi-criteria analysis of bidirectional solar district heating substation architecture," in *Proceedings of SWC2017/SHC2017*, Freiburg, Germany, 2017, pp. 1–11.

[36] I. Sarbu and E. S. Valea, "Energy savings potential for pumping water

in district heating stations," *Sustainability*, vol. 7, no. 5, pp. 5705–5719, 2015.

[37] KSB Aktiengesellschaft, "Pump control / system automation," *KSB Know-how*, vol. 4, 2006.

[38] A. van der Schaft, *L2-Gain and Passivity Techniques in Nonlinear Control*, 3rd ed. Springer International Publishing AG, 2017.

[39] B. Stræde, "Pressure oscillation in district heating installations," Danfoss A/S, 6430 Nordborg, Denmark, 1995.

[40] H. Boysen and J. E. Thorsen, "How to avoid pressure oscillations in district heating systems," Danfoss A/S, Nordborg, 2003.

[41] J. E. Machado, M. Cucuzzella, N. Pronk, and J. M. A. Scherpen, "Adaptive control for flow and volume regulation in multi-producer district heating systems," *IEEE Control Systems Letters*, vol. 6, pp. 794–799, 2022.

APPENDIX I
LIST OF ABBREVIATIONS

DHN	District heating network
DGU	Distributed (heat) generation unit
PHS	Port-Hamiltonian system
ISO-PHS	Input-state-output port-Hamiltonian system
KVL	Kirchhoff's voltage law
KCL	Kirchhoff's current law

APPENDIX II
SYMBOLS DESCRIPTION

$\mathcal{G}, \mathcal{V}, \mathcal{E}$	DHN graph, vertices (Kirchhoff nodes), and edges
$\mathcal{D}, \mathcal{L}, \mathcal{P}$	Edge sets representing DGUs, end-users (loads), and pipes
$\mathcal{N}_c^+, \mathcal{N}_c^-$	Set of incoming and outgoing edges at a node $c \in \mathcal{V}$
μ_i, μ_j	Pressure drop due to nonlinear valve friction in DGUs $i \in \mathcal{D}$ and end-users $j \in \mathcal{L}$
$\lambda_i, \lambda_j, \lambda_l$	Pressure drop due to nonlinear pipe friction in DGUs $i \in \mathcal{D}$, end-users $j \in \mathcal{L}$, and pipes $l \in \mathcal{L}$
J_i, J_j, J_l	Inertia of the volume in hydraulic circuits of DGUs $i \in \mathcal{D}$, end-users $j \in \mathcal{L}$, and pipes $l \in \mathcal{L}$
$C_{\mathrm{R}i}, C_{\mathrm{R}j}$	Elasticity of the hydraulic circuits of DGUs $i \in \mathcal{D}$ and end-users $j \in \mathcal{L}$ summarized at the return side
$C_{\mathrm{S}i}, C_{\mathrm{S}j}$	Elasticity of the hydraulic circuits of DGUs $i \in \mathcal{D}$ and end-users $j \in \mathcal{L}$ summarized at the supply side
$(\cdot)_{\mathrm{P}\alpha}$	Quantity associated to the pressure holding $\alpha = 1$ or the dynamic pump model $\alpha = 2$
$x_{k,m}, d_{k,m}, z_{k,m}$	kth component of the vector $\mathbf{x}$, $\mathbf{d}$ and $\mathbf{z}$ associated with edge $m \in \mathcal{E}$, respectively
$J_{\mathrm{P}\alpha}, R_{\mathrm{P}\alpha}, C_{\mathrm{P}\alpha}$	Black box parameters to approximate the pressure holding and pump dynamics
$\mathrm{col}\,(x_i)_{i \in \mathcal{I}}$	Column vector of real elements x_i ordered according to an index set $\mathcal{I}$